

Effect of gas pressure and electron advection on self-organized structures in DBD micro-plasma

DBD マイクロプラズマの自己組織構造におけるガス圧力と電子移流の効果

Tomohiro Kudo, Kazunobu Fujiwara, Seji Mukaigawa, Koichi Takaki

工藤智広, 藤原一延, 向川政治, 高木浩一

Faculty of Engineering, Iwate University, 4-3-5 Ueda, Morioka, Iwate, 020-8551, Japan

岩手大学工学部, 〒020-8551 岩手県盛岡市上田4-3-5

In this study, we experimentally produced hexagonal disposition filament structures in dielectric barrier discharges (DBDs) and observed the changes due to pressure and electron advection. We used experiments and numerical simulations to investigate the effects of pressure on the hexagonal patterns formed by self-organization in micro-gap DBDs. In simulations with changing advective velocities, the filament diameters were 1.524 mm at 0.00794 m/s and 1.786 mm at 0.952 m/s. In experiments with changing gas flow velocities, the filament diameters were 0.215 mm at 4.8 m/s and 0.479 mm at 19.2 m/s. In other words, diameters increased with increasing flow velocity.

1. Introduction

Plasma organizes autonomously under special dielectric barrier discharge (DBD) conditions, and the discharge also becomes spatially inhomogeneous. Plasma photonic crystals are an anticipated application of this inhomogeneous discharge [1,2]. There is a contribution of gas flow perpendicular to the electric field when an inhomogeneous structure becomes homogenized.

In this study, we considered the effect of electron advection on the formation of self-organized structures. We obtained the diameter of a filament and considered the validity of the experiment by simulating a model that added an advective term to the discharge system.

2. Experimental setup

Figure 1 shows the experimental setup. A microgap was constructed with a dielectric, a spacer, another dielectric, and a driving electrode on a 100 mm × 100 mm copper plate.

The dielectrics and spacer were made of glass with a thickness of 140 μm and a relative permittivity of 6. The width of the flow channel serving as the discharge region was 5 mm. The driving electrode was indium–tin–oxide to enable observation of emissions from the discharge. The introduced gas was six nines (99.9999%) pure He. The buffer area was set up at the upper side of the microchannel for the gas installation. The microchannel was open underneath, where the gas was directly emitted. The gas flow velocity changed in the range of 4.8 m/s to 28.8 m/s. The source voltage was 450 V. The emission upon discharge was observed with an intensified charge-coupled device camera. The applied voltage was measured with a high voltage probe. The current was measured by a Rogowski

coil.

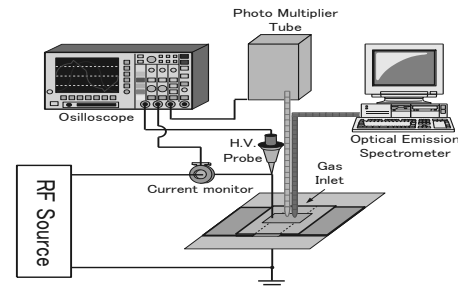


Fig.1 Experimental setup

3. Experimental result

Figure 2 shows the discharge aspects when flow velocity was changed. The flow velocities were (a) 4.8 m/s, (b) 9.6 m/s, (c) 14.4 m/s, (d) 19.2 m/s, (e) 24.0 m/s, and (f) 28.8 m/s. The images at the top show the upper stream of the gas, and that at the bottom shows the lower stream. Many filaments appeared and formed hexagonal structures when the flow velocity was 4.8 m/s. The homogeneous region expanded with an increase in flow velocity. The diameters of the filaments in Figures 2(a)–2(d) were (a) 0.215 mm, (b) 0.396 mm, (c) 0.475 mm, and (d) 0.470 mm. The filament diameter increased with increased flow velocity.

4. Model

Equations (1) and (2) comprise the discharge system reaction diffusion equation [3].

$$\frac{\partial U}{\partial t} = \frac{U_0 - U}{\tau_U} - cNU + D_U \Delta U \quad (1)$$

$$\frac{\partial N}{\partial t} = -\frac{N}{\tau_N} + NU \left[a + b \left(\frac{N}{N+N^*} \right)^2 \right] + D_N \Delta N - v_y \frac{\partial N}{\partial y} \quad (2)$$

Where U is the active factor and N is the depressant factor. U shows the voltage drop of the discharge gap; N shows the charge carrier density of the gap. U and N are represented as a function of time t , at position x, y . τ_U is the time constant of the line, τ_N

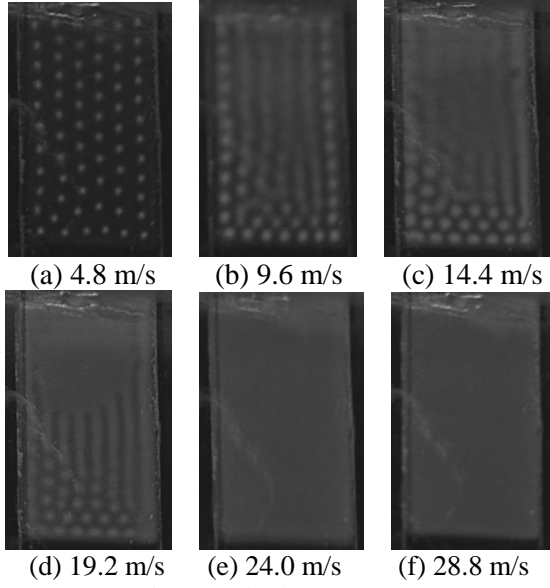


Fig.2 Discharge aspect

is the lifetime of the charge carrier, U_0 is the source voltage, and c is the constant of the discharge gap and is expressed by Equation (3).

$$c = \frac{\epsilon \mu}{\epsilon_0 \epsilon_g (1 + C_b / C_g)} \quad (3)$$

Where e is the charge, μ is the mobility, ϵ_0 the permittivity of the vacuum, ϵ_g is the relative permittivity of He, C_b is the capacity of dielectric barrier, and C_g is the capacity of the gap. a is expanded to $a = 1/\tau_N U_0$ and is the constant that settles the critical voltages that transit from $N(t,x,y) = 0$ to $N(t,x,y) > 0$. b and N^* are the phenomenological parameters of Equation (2). D_U and D_N are the diffusion coefficients of U and N , respectively, and meet the workable condition of the Turing mechanism that states that the depressant factor's diffusion is faster than that of the active factor ($D_U > D_N$). In this simulation, the fixed parameters are $a = 3.4$, $b = 3.4$, $c = 1.64 \times 10^{-4}$ cm²/sec, $\tau_U = 10^{-2}$ sec, $\tau_N = 10^{-3}$ sec, $N^* = 1.5 \times 10^5$ cm⁻², $D_U = 0.625$ cm²/sec, and $D_N = 0.045$ cm²/sec. v_y is the electron flow velocity that moves by gas flow. In our simulation, the flow velocity measures the direction of the y axis. The calculation area is a $-1 < x < 1$, $-1 < y < 1$ square region, and the boundary condition that flux zero is on the boundary of $x = \pm 0$ is a condition in which the incursion flux is equal to the effusion flux (Equation (4)).

$$-D_N \frac{\partial N}{\partial y} + v_y N \Big|_{y=-1} = - \left(D_N \frac{\partial N}{\partial y} - v_y N \right) \Big|_{y=1} \quad (4)$$

The initial condition of U is $U(0,x,y) = 240$ V. The initial condition of N is $N(0,x,y) = 10^6 e^{-(x^2+y^2)/0.001}$ as the regional

perturbation.

5. Simulation result

Figure 3 shows the 2D distribution density plot of $N(t,x,y)$. The flow velocities of (a), (b), (c), and (d) were 0.00794 m/s, 0.0397 m/s, 0.794 m/s, and 0.0952 m/s, respectively. Filaments appeared and formed hexagonal structures over the calculation area. The filament diameters were (a) 1.524 mm, (b) 1.540 mm, (c) 1.746 mm, and (d) 1.786 mm, becoming larger with increased flow velocity. This result cannot be compared directly but is consistent the experimental results.

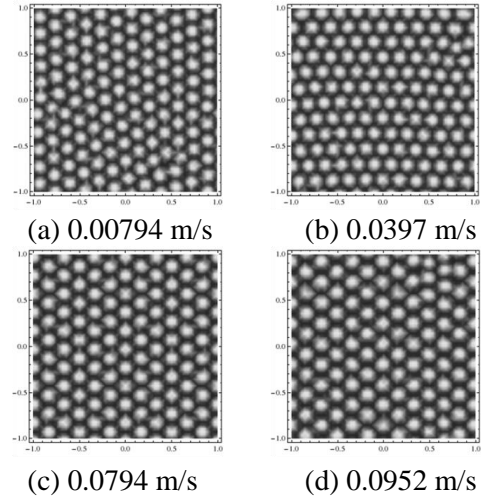


Fig.3 2D distribution plot of $N(t,x,y)$

6. Conclusion

We investigated the effects of pressure and electron advection on the hexagonal patterns formed by self-organization in micro-gap DBDs. We conducted a discharge experiment by changing the flow velocity in microgap DBDs and conducted a numerical simulation using a model that added an advective term to the discharge system. While the dispositions cannot be directly compared, results showed that the diameter of the current filament became larger with increasing flow velocity in both the experiment and simulation; therefore, this model can replicate the disposition of the experiment.

References

- [1] T. Shao, K. Long, C. Zhang, J. Wang, D. Zhang, P. Yan, S. Zhang, "Electrical characterization of dielectric barrier discharge driven by repetitive nanosecond pulses in atmospheric air", Journal of Electrostatics 67, 215-221 2009
- [2] O. Sakai, T. Sakaguchi, and K. Tachibana, "Plasma photonic crystals in two-dimensional arrays of microplasmas", Contrib Plasma Phys.47, No.1-2, pp 96-102 2007
- [3] Yu. A. Astrov and E. V. Beregin, "Polymorphism of condensed phase of dissipative solitons", Technical Physics Letters vol.36 No.7 2010